

4*f* electron delocalization and volume collapse in praseodymium metal

Joseph A. Bradley,^{1,*} Kevin T. Moore,¹ Magnus J. Lipp,¹ Brian A. Mattern,² Joseph I. Pacold,² Gerald T. Seidler,² Paul Chow,³ Eric Rod,³ Yuming Xiao,³ and William J. Evans¹

¹*Condensed Matter and Materials Division, Lawrence Livermore National Laboratory, Livermore, California 94550, USA*

²*Department of Physics, University of Washington, Seattle, Washington 98195-1560, USA*

³*HP-CAT, Geophysical Laboratory, Carnegie Institute of Washington, Argonne, Illinois, 60439, USA*

(Received 7 February 2012; published 30 March 2012)

We study the pressure evolution of the 4*f* electrons in elemental praseodymium metal compressed through several crystallographic phases, including the large volume-collapse transition at 20 GPa. Using resonant x-ray emission, we directly and quantitatively measure the development of multiple electronic configurations with differing 4*f* occupation numbers, the key quantum observable related to the delocalization of the strongly correlated 4*f* electrons. These results provide a high-fidelity test of prior predictions by dynamical mean-field theory, and support the hypothesis of a strong connection between electronic and structural degrees of freedom at the volume-collapse transition.

DOI: [10.1103/PhysRevB.85.100102](https://doi.org/10.1103/PhysRevB.85.100102)

PACS number(s): 61.50.Ks, 71.30.+h, 71.27.+a

Electronic delocalization transitions are of great interest because they denote the onset of large-scale electronic correlations in materials. They occur when tightly bound, atomiclike orbitals begin to mix with orbitals on neighboring lattice sites. Taken to the furthest extent, these atomic orbitals would eventually become single-electron Bloch wave functions, coherently mixed from site to site, and their degenerate energies would split into bands. Between the well-understood atomic limit and the well-understood uncorrelated band limit lie exotic behaviors, including Mott metal-to-insulator transitions,¹ structural volume collapses,^{2–16} hidden orderings,¹⁷ heavy-fermion superconductivity,¹⁸ and anomalous transport and expansion properties.¹⁹ Unfortunately, computations cannot treat all degrees of freedom in systems with strongly correlated electrons, placing a premium on judicious determination of the *important* degrees of freedom, their interactions, and an appropriate quantum mechanical basis. For systems that exhibit delocalization transitions, pressure and temperature can be used to effectively tune the electronic correlations while experimentally measuring quantum observables as the correlation evolves. Such measurements may then be directly compared to theories that treat electron correlations.

Lanthanide materials represent an ideal class of materials for this task. Light rare-earth metals exhibit pressure-driven volume collapses attributable to *f* electron delocalization. Most notable are the elemental metals, Ce, Pr, and Gd. In the vicinity of these phase transitions, the 4*f* electrons take on highly correlated, nonatomic character, making them discordant with many theoretical treatments. Their behavior has been approached by using impurity models,²⁰ by considering static approximations to electron correlation effects on a real lattice,^{21,22} and recently by a fully dynamical treatment of correlations in the lattice using dynamical mean-field theory (DMFT) combined with density functional theory (DFT).^{23,24} DMFT, which is widely considered to be state of the art, offers explicit, testable predictions of the phonon density of states,²⁵ electron coherence,²⁶ and electron occupancy number and weightings as a function of pressure.²³ One technique that can directly test DMFT treatments of electron correlations is resonant x-ray emission spectroscopy (RXES). In this process,

the incident photon energy is chosen to coincide with one of the atomic x-ray absorption edges of the system, enhancing the inelastic scattering cross section. A core hole is made, which is quickly filled by a decaying electron that emits a photon. The emitted photons yield detailed information on the electronic structure of correlated materials, as in the case of the *L* edge of rare-earth materials, where the 4*f* electron occupancy as a function of pressure is revealed.^{3,4,27,28} Such results can be directly compared to DMFT predictions, making a powerful connection between experiment and theory.

The rare-earth metal Pr makes a compelling test case. It exhibits the symmetry evolution dhcp → fcc → distorted-fcc → orthorhombic with a large (~10%) volume-collapse at the distorted-fcc → orthorhombic transformation at 20 GPa.⁹ Through this evolution, the 4*f* electrons go from localized in the low-pressure phases to delocalized in the high-pressure orthorhombic phase, which is the same as α -U—a structure widely agreed on as the prototypical crystal structure of *f* electron materials with one to three delocalized *f* states.²⁹ Thus, the structural signature of crossing a localized-delocalized transition is present. However, previous measurements question this interpretation: No change was observed in the *L*₃-edge x-ray absorption spectroscopy (XAS) profile through the volume-collapse transition. This would indicate either an *f*-count-insensitive delocalization or no delocalization of the *f* electrons at all.³⁰ Such conclusions would be in stark contrast to predictions by DMFT, and would be inconsistent with high-pressure resistance measurements that imply at least a partial delocalization of the 4*f* electrons.^{31–33} This inconsistency demands further investigation.

Here, we go beyond XAS, and present an *L* α RXES determination of 4*f* electron occupancy as a function of pressure in Pr metal. The RXES measurement should be more sensitive than conventional XAS to changes in electron occupancy because conventional XAS is subject to a rather large broadening (~3 eV) due to the short lifetime of the 2*p*_{3/2} core hole. Furthermore, this experiment offers a direct, high-fidelity test for 4*f* delocalization and DMFT predictions. By comparing over a fine grid of pressures spanning from 7 to 32 GPa, our results strongly support DMFT treatment

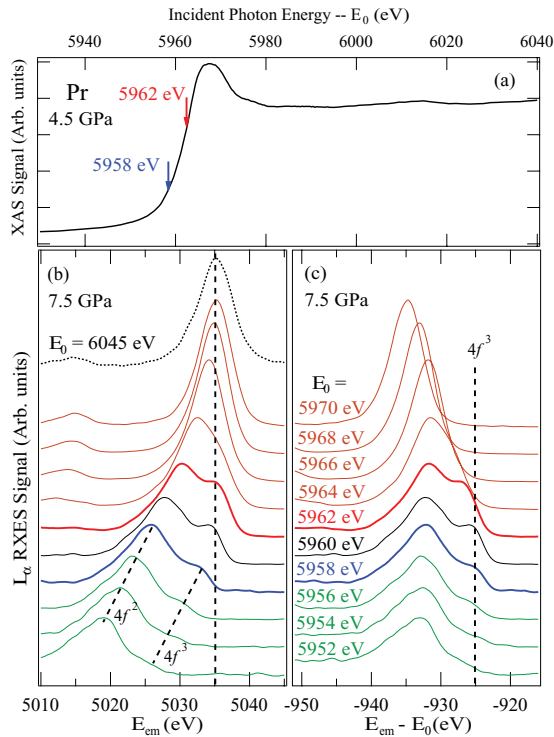


FIG. 1. (Color online) (a) The low-pressure (4.5 GPa) L_3 x-ray absorption edge of elemental Pr. (b) RXES spectra (at various incident energies) from Pr at 7.5 GPa as a function of emitted photon energy. The vertical line is centered on the nonresonant x-ray emission feature. Spectral features corresponding to well-resolved final states of $4f^2$ and $4f^3$ occupancy are labeled. (c) Identical data to that of (b), but set on an energy scale that is constant for features corresponding to a fixed final state. Spectra in (b) and (c) are normalized and offset for clarity of presentation.

of electron correlation across the $4f$ localization transition, putting the theory on firm experimental ground.

All RXES measurements were performed at sector 16 of the Advanced Photon Source. Pr $L\alpha$ RXES spectra were taken using a dispersive, miniature x-ray spectrometer using several flat Ge (331) Bragg analyzers.^{34,35} Incident energies were varied around the excitation energy for the $2p_{3/2}$ electrons, ranging from 5950 to 6040 eV. The net experimental energy resolution, including effects of the incident beam bandwidth, was ~ 1.3 eV. The incident energy calibration was monitored via x-ray absorption through a Cr foil and found to be steady. Samples were pressurized using diamond anvil cells (DAC) with Be gaskets. Because Pr is highly reactive, DAC loading was conducted in a glove box under dry N_2 gas, and Ne was loaded as a pressure-transmitting medium. This loading process was tested by L_3 -edge x-ray absorption at sector 20 of the Advanced Photon Source, and it was seen to yield Pr metal. The focused incident x-ray beam, approximately $30 \times 50 \mu\text{m}$, was fired through the gasket, and the resulting fluorescence photons escaped through the gasket as well.

The Pr $L\alpha$ RXES spectra for various incident x-ray energy (E_0) are shown in Figs. 1(b) and 1(c), at a pressure of 7.5 GPa. For reference, the x-ray absorption spectrum of Pr at 4.5 GPa is also shown in Fig. 1(a). In Fig. 1(b), the spectra are displayed as a function of emitted photon energy

(E_{em}), while in Fig. 1(c), the same spectra are shown as a function of the energy difference $E_{\text{em}} - E_0$. This latter energy scale can be thought of as the energy transferred to the sample after the excitation and emission process (a larger negative number denotes a *greater* energy transfer). In Fig. 1(b), we note two well-separated features with diagonal lines. These correspond to the quantum mechanical weighting of the ground state in terms of atomic configurations with two and three $4f$ electrons, respectively.^{4,27,28,36} Consequently, we label and refer to these features as “ $4f^2$ ” and “ $4f^3$ ” in analogy to this earlier work. It is straightforward to describe the basic sensitivity of $2p$ RXES to $4f$ occupancy. Consider a system with a ground state described as a superposition of atomlike states with differing $4f$ occupancies. After the initial photon is absorbed, the intermediate state excitation is shorter lived than the characteristic fluctuation time for $4f$ occupation, which enforces a fixed $4f$ count. Different $4f$ counts have different nuclear screening and thus affect the energy transferred to the system in its final state—i.e., after the intermediate state decays by emitting a photon ($3d \rightarrow 2p$). These variations in final state energy are visible as shifted (and superimposed) x-ray emission lines, and so the relative intensities of the emission lines correspond to the relative quantum mechanical weightings of the different f occupancy. This heuristic description has been put on firm footing using impurity model calculations.⁴

Since there may be mixing between different occupancies in the intermediate and final states, the precise correspondence between feature intensity and occupancy weighting would require a detailed calculation. Here we make the simplifying assumption that the correspondence is linear through the small range (10%–30%) of $4f^3$ weight we observe, with the constant of proportionality determined by the experiment. Precise accounts of the relationship between spectral feature size and f occupancy show mild nonlinearities on the scale of interest,³⁷ meaning some mild systematic deviation is possible, and detailing this would be a welcome avenue for future theoretical work.

One subtlety remains: To accurately measure the $4f$ electron occupation, an appropriate incident energy must be chosen. This is because the heuristic description proffered above breaks down as the excited photoelectron begins exploring states that are less strongly localized. Again, consider Fig. 1(b): At low incident energies the spectra consist of clear and largely unchanging double-peaked excitation structures, indicative of a pair of well-resolved final states. The x-ray emission energies of these peaks shift with the incident x-ray energy (so-called “Raman” shifting), because for fixed final states, the energy transferred to the system must remain constant.²⁷ The energy scale utilized in Fig 1(c) now becomes quite useful, because it aligns these Raman-shifting features vertically. At around $E_0 = 5960$ eV, the higher-energy feature begins to deviate from the expected Raman shift, so the energy transferred to the system after deexcitation is no longer constant. This indicates a somewhat uncorrelated excited photoelectron, able to take on excess kinetic energy and alter the total energy transferred to the sample. This understanding is further supported by Fig. 1(b), which shows that at $E_0 = 5962$ eV the higher-energy line emits photons precisely at the nonresonant emission energy, meaning the feature dispersion

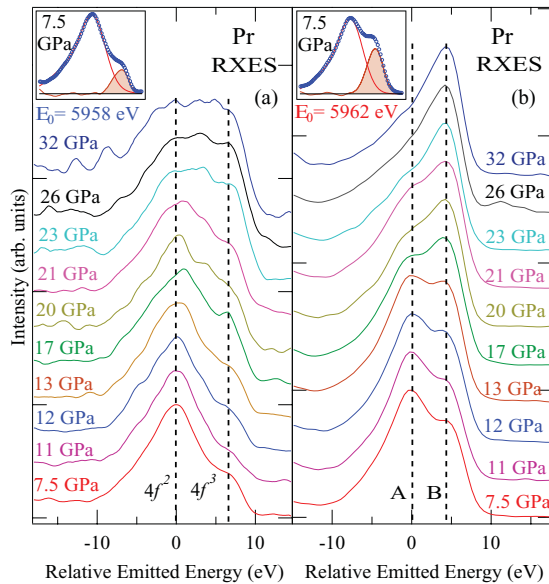


FIG. 2. (Color online) (a) RXES spectrum as a function of pressure taken at $E_0 = 5958$ eV. The inset displays the deconvolution procedure at 7.5 GPa. (b) RXES spectra taken at $E_0 = 5962$ eV. Note the smaller feature separation, signifying that the simple connection to $4f$ occupancy is invalid, as we discuss in the text. The spectra in (a) and (b) are offset and presented in energy units relative to the main line of the spectrum. Both of these are for clarity of presentation.

changes precisely at the onset of the “fluorescence” regime.²⁷ The conclusion is that at $E_0 = 5962$ eV, while the line with emission energy $E_{em} = 5035$ eV may have a component that comes from the desired localized final state, it also has another component that is from a final state containing an extended photoelectron. This resonance could also be further contaminated by interference effects between the two relevant intermediate channels, resulting in a mixture of undetermined $4f^2$ and $4f^3$ character.

Keeping the difficulties expected for the spectra taken at 5962 eV in mind, in Fig. 2 we present the Pr $L\alpha$ RXES spectrum as a function of pressure from 7.5 to 32 GPa. Each spectrum is normalized to have equivalent intensity at the peak. To emphasize the evolution of the RXES line shape, rather than relative motion of bands or other effects, we present our results shifted to a common energy scale where the $4f^2$ features are aligned. In Fig. 2(a), with incident energy $E_0 = 5958$ eV, two well-separated features are visible (occurring at ~ 5024 and ~ 5031 eV).

Visual examination of Fig. 2(a) already establishes a main qualitative result of this work: the observation of discontinuity in the electronic-state evolution through the volume-collapse. At 7.5 GPa in Fig. 2(a) the $4f^2$ peak is clearly dominant, while at 32 GPa the two peaks are much closer in intensity. Between these two pressures the intensities vary due to the change in electron occupancy weightings. While the variation up to 21 GPa is subtle and continuous, the final three spectra taken at 23, 26, and 32 GPa are clearly of different character than the lower-pressure spectra. This discontinuity can be quantified, though the nontrivial line shape of the features and the noise level of the data do complicate the fitting routine for the data at 5958 eV. The general program is to

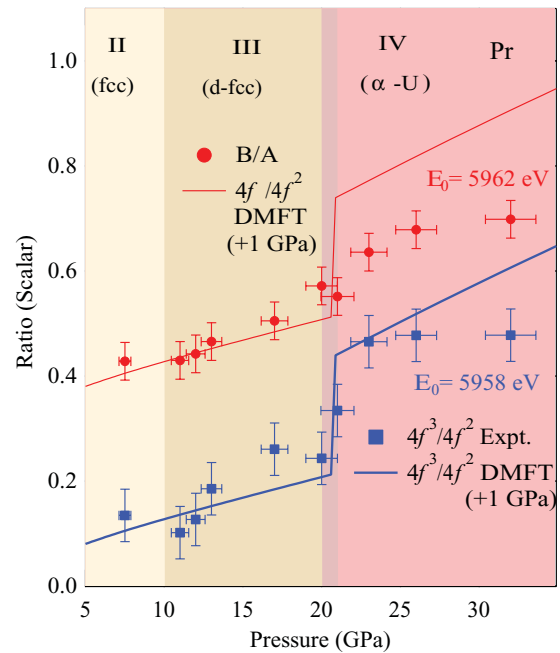


FIG. 3. (Color online) Comparison of experimental and theoretical $4f^3$ to $4f^2$ occupancy ratios as a function of pressure for Pr metal. The square data points (blue) are derived from deconvolution of the RXES spectra at $E_0 = 5958$ eV, and compare favorably to theory. The round data points (red) come from the ratio of the A and B features in the $E_0 = 5962$ eV data and are expected to disagree with predictions, as is shown here. The high-pressure deviation between the 5958 eV data and theory and the 1 GPa shift of the theory are explained in the text. $E_0 = 5962$ eV data are offset for clarity.

extract the $4f^2$ and $4f^3$ feature integral intensities and take their ratio. To do so, three Gaussian forms were fit to the 7.5 GPa data (two for the $4f^2$ feature and a single Gaussian for the $4f^3$). The low-pressure fit to the $4f^2$ feature was then subtracted from each higher-pressure data set, and the residual was integrated in the neighborhood of the $4f^3$ feature. The low-pressure fit to the $4f^2$ feature fits the higher-pressure data very well, as judged by the residuals. For comparison, an identical procedure was applied to the data taken at $E_0 = 5962$ eV [Fig. 1(c)], where the onset of the fluorescence regime is expected to make the connection between spectral weight and $4f$ occupancy problematic. Uncertainties were estimated for the $E_0 = 5962$ eV by comparing the results of this fitting procedure to those obtained from fitting independent Gaussian forms to spectra at all pressures. This estimate also formed the basis for the uncertainty in the $E_0 = 5958$ eV fit results, though to improve the estimate it was combined through error propagation with an uncertainty derived from the higher noise level in these data.

The extracted peak intensity ratios are displayed in Fig. 3, shown as functions of pressure and superimposed against the crystallographic phases of Pr. Here, we present results derived from measurements at both incident energies, to emphasize that selecting the wrong incident energy gives misleading results. The most important data in this plot are the measurements of the $4f^3$ to $4f^2$ ratio, which we compare directly to DMFT predictions. These data are derived from the emission

spectra taken at $E_0 = 5958$ eV, and they are shown as square markers with associated error bars. The solid curve is the ratio of occupancy weightings as predicted by DMFT.²³ The DMFT results have been presented in terms of pressure, instead of their native description as a function of unit cell volume, by use of published data on the Pr equation of state.⁸ We compare the experiment to theory using a single multiplicative scale factor, which is tantamount to the assumption of a linear relation between f electron configuration weight and feature size, as discussed above. Doing so, we find strong agreement, including a clear step in the f electron occupancy weightings due to the volume-collapse. For contrast, the circular data markers show the pressure evolution of the integrated intensity ratio from the spectra taken at $E_0 = 5962$ eV. Here, the inclusion of final states with an uncorrelated photoelectron complicates the connection between measured intensities and configuration weightings, causing the observed disagreement between the calculation and the $E_0 = 5962$ eV results.

Even for the results at $E_0 = 5958$ eV, there are some observable differences that should be discussed between the experimentally measured $4f$ occupation ratio and the predicted ratio in Fig. 3. First, the transition—and hence the step in $4f$ occupancy—is expected at 20 GPa, but appears at ~ 21 GPa. Sluggishness in this transition would be a consequence of metastability and has been observed before,⁹ but the apparent late onset of the transition could also be due to the fact that the volume probed by the x-ray beam is on the outermost portion of the sample near the gasket. One would therefore expect the pressure at the beam spot to be somewhat lower than that indicated by the ruby monitors, which were farther inside the gasket hole. To account for this and clarify presentation, the DMFT prediction was shifted everywhere by 1 GPa, as noted in the figure. For the same reason, the dividing line between Pr III and Pr IV is indicated as a band between 20 and 21 GPa, while in theory this should be a sharp line just under 20 GPa. This is a purely experimental issue. Second, above the volume-collapse pressure, the theory may overestimate the amount of $4f^3$ character in the electronic ground state. This overestimate is expected because the particular DMFT calculation featured here forced a zero weighting of configurations with more than three $4f$ electrons.²³ Because of the higher degree of delocalization, the $4f^4$ and higher configurations will in reality become occupied at high pressure, which the calculation mistakenly counts as $4f^3$ weight. Therefore, ignoring these higher occupancies gives a spuriously high $4f^3$ configuration weight above the volume-collapse, driving the calculated $4f^3$ to $4f^2$ ratio up at highest pressure.

Structural transformations, especially large volume changes, are thought to be intimately tied to abrupt changes in the electronic structure. This has been seen for martensitic transformations³⁸ and Ce-based materials.³⁹ However, as a rule for f electron systems, this hypothesis is contentious. Previous work on Pr metal seemed to suggest totally inert $4f$ electron behavior,³⁰ which would imply a very different mechanism for the Pr volume-collapse. Furthermore in elemental Am metal, experiment and theory (in this case, DFT) have both supported *unchanging* $5f$ count up to 23 GPa—even through four phases with varying f electron localization (Am I-IV)^{40,41}—in contrast to the DMFT prediction of a developing admixture of f^7 and f^6 states.²⁵

In this uncertain context, the work presented here demonstrates the intimate connection between the $4f$ electronic structure and the volume-collapse using a fine mesh of data points across a pressure-driven transformation, validating the $4f$ delocalization as described in the DMFT picture. Our data monitor the $4f$ states while they make the transition from localized and nonbonding to delocalized and bonding, focusing on the regime of strong electron correlations. Pr is an important test case, since the evolution from fcc into a complex, lower-symmetry structure is a general motif in rare-earth systems and has been tied to $4f$ delocalization.⁴² While the question of generality of $4f$ delocalization at the volume-collapse in the rare earths remains open, the present results will both motivate further studies and also serve as an important anchor in future discussions of $4f$ and $5f$ delocalization.

ACKNOWLEDGMENTS

The authors thank Andy McMahan and Corwin Booth for helpful discussions. This work was performed under the auspices of the U.S. Department of Energy by Lawrence Livermore National Laboratory under Contract No. DE-AC52-07NA27344. G.T.S. acknowledges support from the U.S. Department of Energy under Contract No. DE-SC0002194. Portions of this work were performed at HPCAT (Sector 16) and PNC/XSD, Advanced Photon Source (APS), Argonne National Laboratory. HPCAT is supported by CIW, CDAC, UNLV, and LLNL through funding from DOE-NNSA, DOE-BES, and NSF. PNC/XSD facilities at the Advanced Photon Source, and research at these facilities, are supported by the DOE BES, NSERC, the University of Washington, Simon Fraser University, and the Advanced Photon Source. APS is supported by DOE-BES, under Contract No. DE-AC02-06CH11357.

*bradley41@llnl.gov

¹M. Imada, A. Fujimori, and Y. Tokura, *Rev. Mod. Phys.* **70**, 1039 (1998).

²A. K. McMahan, *Phys. Rev. B* **72**, 115125 (2005).

³B. R. Maddox, A. Lazicki, C. S. Yoo, V. Iota, M. Chen, A. K. McMahan, M. Y. Hu, P. Chow, R. T. Scalettar, and W. E. Pickett, *Phys. Rev. Lett.* **96**, 215701 (2006).

⁴J.-P. Rueff, J.-P. Itie, M. Taguchi, C. F. Hague, J.-M. Mariot, R. Delaunay, J.-P. Kappler, and N. Jaouen, *Phys. Rev. Lett.* **96**, 237403 (2006).

⁵M. J. Lipp, D. Jackson, H. Cynn, C. Aracne, W. J. Evans, and A. K. McMahan, *Phys. Rev. Lett.* **101**, 165703 (2008).

⁶H. K. Mao, R. M. Hazen, P. M. Bell, and J. Wittig, *J. Appl. Phys.* **52**, 4572 (1981).

⁷S. R. Evans, I. Loa, L. F. Lundegaard, and M. I. McMahon, *Phys. Rev. B* **80**, 134105 (2009).

⁸G. N. Chesnut and Y. K. Vohra, *Phys. Rev. B* **62**, 2965 (2000).

⁹B. J. Baer, H. Cynn, V. Iota, C.-S. Yoo, and G. Shen, *Phys. Rev. B* **67**, 134115 (2003).

- ¹⁰N. C. Cunningham, N. Velisavljevic, and Y. K. Vohra, *Phys. Rev. B* **71**, 012108 (2005).
- ¹¹J. Akella and G. S. Smith, *J. Less-Common Met.* **116**, 313 (1986).
- ¹²F. Decremps, L. Belhadi, D. L. Farber, K. T. Moore, F. Occelli, M. Gauthier, A. Polian, D. Antonangeli, C. M. Aracne-Ruddle, and B. Amadon, *Phys. Rev. Lett.* **106**, 065701 (2011).
- ¹³K. T. Moore, L. Belhadi, F. Decremps, D. L. Farber, J. A. Bradley, F. Occelli, M. Gautier, A. Polian, and C. M. Aracne-Ruddle, *Acta Mater.* **59**, 6007 (2011).
- ¹⁴S. Heathman, R. G. Haire, T. Le Bihan, A. Lindbaum, K. Litfin, Y. Meresse, and H. Libotte, *Phys. Rev. Lett.* **85**, 2961 (2000).
- ¹⁵S. Heathman, R. G. Haire, T. Le Bihan, A. Lindbaum, M. Idiri, P. Normile, S. Li, R. Ahuja, B. Johansson, and G. H. Lander, *Science* **309**, 110 (2005).
- ¹⁶P. Soderlind, K. T. Moore, A. Landa, B. Sadigh, and J. A. Bradley, *Phys. Rev. B* **84**, 075138 (2011).
- ¹⁷P. Chandra, P. Coleman, J. A. Mydosh, and V. Tripathi, *Nature* **417**, 831 (2002).
- ¹⁸C. Pfeleiderer, *Rev. Mod. Phys.* **81**, 1551 (2009).
- ¹⁹K. T. Moore and G. van der Laan, *Rev. Mod. Phys.* **81**, 235 (2009).
- ²⁰J. W. Allen and R. M. Martin, *Phys. Rev. Lett.* **49**, 1106 (1982).
- ²¹C. M. Aerts, P. Strange, M. Horne, W. M. Temmerman, Z. Szotek, and A. Svane, *Phys. Rev. B* **69**, 045115 (2004).
- ²²P. Soderlind, *Phys. Rev. B* **65**, 115105 (2002).
- ²³A. K. McMahan, R. T. Scalettar, and M. Jarrell, *Phys. Rev. B* **80**, 235105 (2009).
- ²⁴G. Kotliar, S. Y. Savrasov, K. Haule, V. S. Oudovenko, O. Parcollet, and C. A. Marianetti, *Rev. Mod. Phys.* **78**, 865 (2006).
- ²⁵S. Y. Savrasov, K. Haule, and G. Kotliar, *Phys. Rev. Lett.* **96**, 036404 (2006).
- ²⁶C. A. Marianetti, K. Haule, G. Kotliar, and M. J. Fluss, *Phys. Rev. Lett.* **101**, 056403 (2008).
- ²⁷J.-P. Rueff and A. Shukla, *Rev. Mod. Phys.* **82**, 847 (2010).
- ²⁸J.-P. Rueff, C. F. Hague, J.-M. Mariot, L. Journel, R. Delaunay, J.-P. Kappler, G. Schmerber, A. Derory, N. Jaouen, and G. Krill, *Phys. Rev. Lett.* **93**, 067402 (2004).
- ²⁹P. Soderlind, O. Eriksson, B. Johansson, J. M. Willis, and A. M. Boring, *Nature* **374**, 524 (1995).
- ³⁰J. Roehler and R. Luebbbers, *Physica B* **206-7**, 368 (1995).
- ³¹J. J. Hamlin, J. R. Jeffries, G. Samudrala, Y. K. Vohra, S. T. Weir, D. A. Zocco, and M. B. Maple, *Phys. Rev. B* **84**, 033101 (2011).
- ³²N. Tateiwa, A. Nakagawa, K. Fujio, T. Kawae, and K. Takeda, *J. Alloys Compd.* **408-412**, 244 (2006).
- ³³N. Velisavljevic, K. M. MacMinn, Y. K. Vohra, and S. T. Weir, *Appl. Phys. Lett.* **84**, 927 (2004).
- ³⁴B. Dickinson, G. T. Seidler, Z. W. Webb, J. A. Bradley, K. P. Nagle, S. M. Heald, R. A. Gordon, and I. M. Chou, *Rev. Sci. Instrum.* **79**, 123112 (2008).
- ³⁵J. I. Pacold, J. A. Bradley, B. A. Mattern, M. J. Lipp, G. T. Seidler, P. Chow, Y. Xiao, E. Rod, B. Rusthoven, and J. Quintana, *J. Synchrotron Radiat.* **19**, 245 (2012).
- ³⁶F. Bartolome, J. M. Tonnerre, L. Seve, D. Raoux, J. Chaboy, L. M. Garcia, M. Krisch, and C. C. Kao, *Phys. Rev. Lett.* **79**, 3775 (1997).
- ³⁷O. Gunnarsson and K. Schönhammer, *Phys. Rev. B* **28**, 4315 (1983).
- ³⁸G. Jakob, T. Eichhorn, M. Kallmayer, and H. J. Elmers, *Phys. Rev. B* **76**, 174407 (2007).
- ³⁹Q. S. Zeng, V. V. Struzhkin, Y. Z. Fang, C. X. Gao, H. B. Luo, X. D. Wang, C. Lathe, W. L. Mao, F. M. Wu, H.-K. Mao, and J. Z. Jiang, *Phys. Rev. B* **82**, 054111 (2010).
- ⁴⁰S. Heathman, J.-P. Rueff, L. Simonelli, M. A. Denecke, J. C. Griveau, R. Caciuffo, and G. H. Lander, *Phys. Rev. B* **82**, 201103 (2010).
- ⁴¹P. Soderlind and A. Landa, *Phys. Rev. B* **72**, 024109 (2005).
- ⁴²A. K. McMahan, C. Huscroft, R. T. Scalettar, and E. L. Pollock, *J. Comput.-Aided Mater. Des.* **5**, 131 (1998).